JACS
JOURNAL OF THE AMERICAN CHEMICAL SOCIETY

ARTICLE

pubs.acs.org/JACS

Self-Regulating Enzyme−Nanotube Ensemble Films and Their Application as Flexible Electrodes for Biofuel Cells

Takeo Miyake,[†,§] Syuhei Yoshino,[†] Takeo Yamada,[‡,§] Kenji Hata,[‡,§] and Matsuhiko Nishizawa*[,†,§]

[†]Department of Bioengineering and Robotics, Tohoku University, 6-6-1 Aramaki Aoba, Aoba-ku, Sendai 980-8579, Japan

[‡]Nanotube Institute of Advanced Industrial Science and Technology (AIST), Tsukuba Central 5, 1-1-1 Higashi, Tsukuba, Ibaraki 308-8565, Japan

[§]Core Research for Evolutional Science and Technology (CREST), Japan Science and Technology Agency (JST), Tokyo 102-0075, Japan

Supporting Information

ABSTRACT: Nanostructured carbons have been widely used for fabricating enzyme-modified electrodes due to their large specific surface area. However, because they are random aggregates of particular or tubular nanocarbons, the postmodification of enzymes to their intrananospace is generally hard to control. Here, we describe a free-standing film of carbon nanotube forest (CNTF) that can form a hybrid ensemble with enzymes through liquid-induced shrinkage. This provides in situ regulation of its intrananospace (inter-CNT pitch) to the size of enzymes and eventually serves as a highly active electrode. The CNTF ensemble with fructose dehydrogenase (FDH) showed the oxidation current density of 16 mA cm^{-2} in stirred 200 mM fructose solution. The power density of a biofuel cell using the FDH−CNTF anode and the Laccase−CNTF cathode reached 1.8 mW cm^{-2} (at 0.45 V) in the stirred oxygenic fructose solution, more than 80% of which could be maintained after continuous operation for 24 h. Application of the free-standing, flexible character of the enzyme−CNTF ensemble electrodes is demonstrated via their use in the patch or wound form.

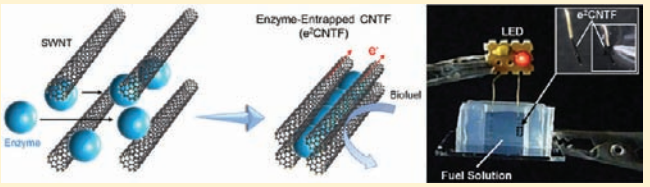

INTRODUCTION

Enzyme-modified electrodes are core components of bioelectronic devices, such as biofuel cells, which have attracted attention as safe power sources, generating electricity from natural fuels, like sugars and alcohols.[1−13] A variety of nanoengineered carbon electrodes for biofuel cells have recently been developed in rapid succession. The carbon nanotube (CNT)-based microfiber electrode is a cutting-edge example that improves a glucose biofuel cell to achieve a power of 0.74 mW cm^{-2} even in physiological, quiescent conditions.[11] Another noteworthy development is the careful control of the intrapore size of carbon cryogel that resulted in a high-power fructose fuel cell producing 0.85 mW cm^{-2} under stirred conditions.[12] The optimized nanopores can be expected to support the activity and the stability of enzymes.[14] However, all attempts to incorporate nanoengineered carbon electrodes have focused on prestructuring electrodes before enzyme modification. This is because the process for engineering carbon is bioincompatible due to the use of organic solvents or heating. If the nanostructure of the electrode can be regulated in response to the enzyme to be immobilized, then the resultant enzymatic ensemble would avoid the difficulty in postmodification of enzymes.

We present here a method to achieve ideal enzyme electrodes having suitable intrananospace automatically regulated to the size of enzymes. We utilize a carbon nanotube forest (CNTF) consisting of extremely long (∼1 mm) single-walled CNTs,[15] which can be handled with tweezers, as a 100% binder-free carbon film. When liquids are introduced into the as-grown CNTF (CNTs with a pitch of 16 nm) and dried, the CNTF shrinks to a near-hexagonal close-packed structure (CNTs with a pitch of 3.7 nm) because of the surface tension of the liquids.[16,17] By using an enzyme solution as the liquid, the CNTF is expected to dynamically entrap the enzymes during the shrinkage, as illustrated in Figure 1. This "in-situ regulation" approach has led to reproducible activity of enzyme electrodes, to the first free-standing flexible character, and to high-power density biofuel cells.

EXPERIMENTAL SECTION

Preparation of Enzyme−Nanotube Ensemble Electrodes.

CNTF was synthesized in a 1-in. tube furnace by water-assisted chemical vapor deposition at 750 °C with a C_2H_4 carbon source and an Al_2O_3 (10 nm)/Fe (1 nm) thin-film catalyst grown on silicon wafers.[15,16] We used He with H_2 as the carrier gas [total flow 1000 standard cubic centimeters per minute (sccm)] at 1 atm with a controlled amount of water vapor with ethylene (100 sccm) for 10 min. The synthesized CNTF (1 mm × 1 mm) could be pulled from the substrate with tweezers (Supporting Information, Figure S1). The film thickness was set to 4 and 12 or 20 μm by the width of line-patterns of the catalyst. The CNTF film

Received: January 5, 2011
Published: March 10, 2011

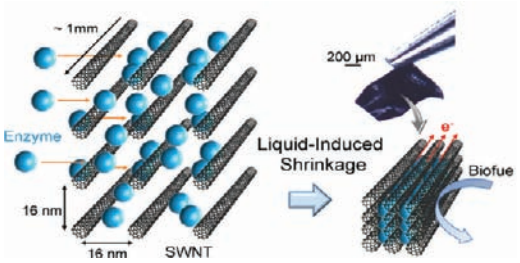

Figure 1. Schematic diagram of enzyme entrapment inside a CNTF by liquid-induced shrinkage. The photograph shows a free-standing enzyme−CNTF ensemble film that can be manipulated with tweezers.

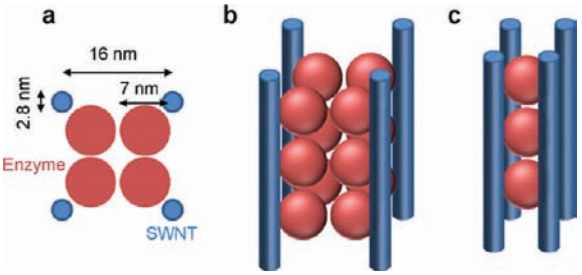

Figure 2. (a and b) Illustrations of as-grown CNTF whose void volume is fully occupied by 7 nm diameter globular enzyme molecules. (c) Illustration of the linear arrangement of the enzymes trapped between the shrunk CNTF.

was evaluated by the Brunauer−Emmett−Teller (BET) analysis of N_2 adsorption and the cyclic voltammetry in McIlvaine buffer (pH 5.0) at 10 mV s^{-1}; the resulting specific surface area and the specific capacitance of the film were approximately 1300 m^2 g^{-1} and 400 F g^{-1}, respectively. The calculated capacitance per effective surface area is thus ca. 30 μF cm^{-2} in agreement with that reported for highly oriented pyrolytic graphite (HOPG).[18]

We used two model enzymes: D-fructose dehydrogenase (FDH; EC 1.1.99.11, 169.9 U mg^{-1}, ca. 140 kDa, from *Gluconobacter*, purchased from Toyobo Enzyme Co.) and laccase (LAC; EC 1.10.3.2, 108 U mg^{-1}, ca. 60 kDa, from *Trametes* sp, purchased from Daiwa Kasei Co.), which can directly catalyze the oxidation of D-fructose and the reduction of dioxygen, respectively.[12] The FDH was used as received without further purification. The LAC was purified by anion exchange chromatography with a DEAE−Toyopearl column.[12] The size of the FDH can be assumed similar to that of 160 kDa glucose oxidase (7 × 5.5 × 8 nm).[19] In fact, the atomic force microscopy (AFM) showed ca. 7 nm bumpy structure for an FDH-adsorbed surface.[20] On the other hand, the LAC has dimensions of 6.5 × 5.5 × 4.5 nm.[21]

The CNTF film was first treated by 0.1% Triton X-100 and then immersed in a stirred McIlvaine buffer (pH 5.0) containing FDH for 1 h to introduce enzymes into its void space. After being washed three times, the CNTF film was placed on a carbon paper and dried in air, typically for 15 min. For cathode preparation, the CNTF film was immersed in 0.25 mg mL^{-1} (4.3 μM) LAC in McIlvaine buffer (pH 5.0) and stirred for 10 min, followed by drying on a carbon paper.

Quantitative Analysis of the Entrapped Enzymes. The enzyme-immobilized CNTF film was washed and immersed in 20 mM sodium phosphate buffer (pH 9.3) containing 0.1 M sodium borate and 1% sodium cholate and dispersed with an ultrasonic homogenizer for 15 min. The FDH in the dispersion was then analyzed using a C-6667 Protein Quantitation Kit (Molecular Probes), using 5 mM (3-(4-carboxybenzoyl)-quinoline-2-carboxaldehyde) (ATTO-TAG CBQCA) and 20 mM KCN to label the enzyme with CBQCA. After 1.5 h of incubation, the fluorescent intensity was measured by a luminescent image analyzer system (Fuji Photo Film, LAS-3000 mini), and the amount of enzyme was determined by referencing a calibration curve.

Theoretical Prospect of FDH Content inside CNTF. The previous structural analysis of the as-grown CNTF revealed a mean tube diameter of 2.8 nm by transmission electron microscopy (TEM) and an intertube pitch of 16 nm by X-ray diffraction (XRD).[16,17] If we assume that FDH is a 7 nm diameter globe, four FDHs can enter the void space surrounded by 16 nm pitched CNTs (Figure 2a and b). The number of enzymes (N_{enz}) entrapped in a 12 μm thick CNTF is estimated by the following equation: $N_{enz} = 4\,(H/r)\,(S/U)$, where H = 1.0 mm (CNT length), $r = 7.0 \times 10^{-6}$ mm (FDH diameter), $S = 12 \times 10^{-3}$ mm^2 (cross-sectional area of CNTF sheet), and $U = 2.6 \times 10^{-10}$ mm^2 (the area of the void space surrounded by 16 nm pitched CNTs). The entrapped mass (6.2 μg) is derived by multiplying N_{enz} by the molecular weight (140 kD)/Avogadro's constant. On the other hand, as we explain later in the Results and Discussion Section, the best performance of FDH−CNTF ensemble was obtained by the film containing ca. 1.5 μg FDH (one-quarter of the limiting value, 6.2 μg) (Figure 2c). Note these arguments are based on the assumption that FDH is a 7 nm diameter globe.

Electrochemical Measurements. The enzyme−CNTF ensemble film, anchored at the edge with SUS316L fine tweezers, was analyzed by a three-electrode system (BSA, 730C electrochemical analyzer) in stirred solutions using a Ag/AgCl reference and a platinum counter electrode. The catalytic currents of enzyme−CNTF ensemble films did not significantly decrease when the film was attached to a planner electrode (Supporting Information, Figure S2). We therefore used the area of one side of the film for the calculation of the current and power densities. The performance of a biofuel cell constructed from an FDH-based anode and an LAC-based cathode was evaluated on the basis of the cell voltage upon changing the external resistance between 1 kΩ and 2 MΩ (1.0, 5.1, 10.8, 15.8, 24.5, 35.3, 55.3, 100, 196, 500, 1000, and 2000 kΩ) at the time step of 60 s. Unless otherwise indicated, the electrochemical measurements were carried out at room temperature (25 °C). Although the apparent Michaelis−Menten constant ($K_{m,app}$) of the entrapped FDH is around 10 mM as we estimated later, we used 200 mM fructose solution in order to evaluate the cell performance in the high enough concentration of fuel and to compare the performance with previous works[12] under similar conditions.

LED Device Experiments. The LED device consisted of a charge pump IC (S-882Z20, input voltage [0.3−3 V), output voltage (V_{IC}, 2 V)], a 1 μF ceramic capacitor (C), and a red LED. The interval of the LED blink is the time required to charge the capacitor, which is described by

$$t = \frac{J}{P} = \frac{\frac{CV_{IC}^2}{2} - \frac{CV_{LED}^2}{2}}{I \times V_{cell}} \quad (1)$$

where J is the practical energy for the LED device operation, P is the cell power, V_{LED} is the operation voltage (1.6 V) of the LED, I is the cell current, and V_{cell} is the cell voltage; thus, the time interval (t) is inversely proportional to the power of the biofuel cell.

RESULTS AND DISCUSSION

Entrapment of Enzymes inside Self-Regulating Nanostructure of CNTF Films. The initial step of the entrapment process depends on sufficient loading of enzymes inside the as-grown 16 nm pitch CNTF film. As shown in Figure 3a, the in situ monitoring of electrocatalytic activity of the CNTF films on soaking in a buffer containing 3 mg mL^{-1} FDH with 200 mM D-fructose showed currents corresponding to their thickness (80

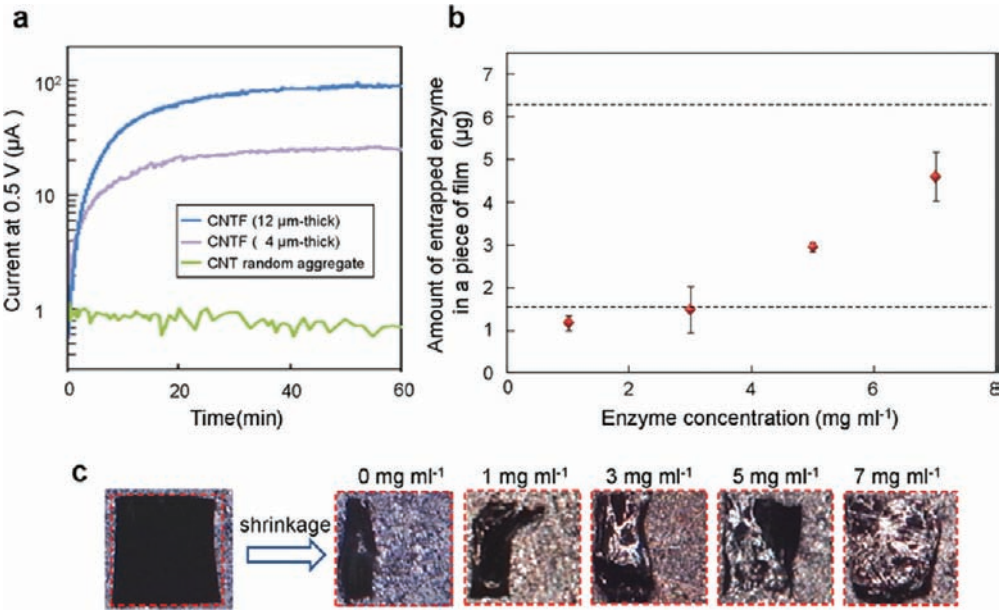

Figure 3. (a) The monitoring of the oxidation current at 0.5 V vs Ag/AgCl in a stirred McIlvaine buffer (pH 5.0) containing 3 mg mL^{-1} FDH and 200 mM fructose for the 4 and 12 μm thick CNTF films (1 × 1 mm), and a random CNT aggregate prepared by casting a CNTs' dispersion on an 1 × 1 mm Au electrode. (b) The relationship between the amount of entrapped FDH inside a piece of 12 μm thick CNTF film and the concentration of FDH solution in which the CNTFs were soaked for 1 h before the shrinkage. The experiments were carried out three times for each condition. (c) Photographs of CNTF films shrunk after soaking in different concentrations of FDH. For reference, the dashed square measures 1 × 1 mm.

μA for 12 μm thick film and 25 μA for 4 μm thick film), indicating that the FDH molecule can entirely penetrate inside the CNTF films. On the other hand, the catalytic activity of the conventional random CNT electrode, which was prepared by casting a CNTs' dispersion, remained around 1 μA despite having a large effective surface area comparable to that of the 4 μm thick CNTF film (both showed capacitance per geometric area of around 5 mF cm^{-2}). The results obtained from the random CNT electrode demonstrate the general difficulty in postmodification of enzymes to the prestructured nanocarbon electrodes, which will be addressed by the present "in-situ regulation" approach.

The content of FDH inside a CNTF film was controllable by the concentration of FDH solution in which the as-grown CNTF films were soaked for 1 h (Figure 3b). The FDH content increased toward the theoretical limiting value (6.2 μg), at which the void volume of as-grown CNTF is fully occupied by FDH (Figure 2). Such controlled entrapment of enzymes can be also examined via the degree of CNTF shrinkage (Figure 3c). Typically, the CNTF film without enzymes shrank to one-quarter of its original area; the CNTF film treated with 3 mg mL^{-1} FDH solution shrank to one-half of the original. The degree of shrinkage also depended on the size of enzyme. For example, a smaller enzyme, laccase, led to shrinkage to one-third of the original area. These results support our methodology, which induces in situ regulation of intrananospace of CNTF by the amount and size of entrapped enzymes. We refer to the enzyme-entrapped CNTF as "e^2CNTF". The enzyme-containing CNTF before shrinkage (before drying), in which enzymes simply adsorbed on CNTs' sidewall, is denoted as "eCNTF".

Electrocatalytic Activity of Enzyme−CNTF Ensembles. The FDH−CNTF ensembles prepared using 3 mg mL^{-1} FDH solution exhibited superior electrocatalytic activity for fructose oxidation in stirred conditions (Figure 4a). The current density of the eCNTF film reached 8 mA cm^{-2} at 0.6 V. In addition, the shrinkage of the area to one-half of the original (see Figure 3c for 3 mg mL^{-1}) boosted the current density by a factor of 2, ca. 16 mA cm^{-2}, indicating that the eCNTF can shrink to the e^2CNTF without significant loss of enzyme activity. Even in quiescent conditions, the current density reached 11 mA cm^{-2} at 0.6 V (Supporting Information, Figure S3). These high current densities of e^2CNTF films indicate an effective interfacing of the enzymes with the large intrasurface of the shrunken CNTF films. In contrast, probably due to the limited loading of enzymes, the conventional random CNT electrode showed a low current density of only ~0.4 mA cm^{-2} (not shown), in agreement with previous reports of conventional CNT aggregate-based enzyme electrodes.[22,23]

The electrode performance depended on the concentration of FDH solution used for preparing e^2CNTFs, as shown in Figure 4b. Among the conditions we studied, the best performance was reproducibly obtained from the e^2CNTF electrode prepared from 3 mg mL^{-1} FDH solution, which contains ca. 1.5 μg FDH (see Figure 3b). This value of FDH content represents one-quarter of the limiting value (6.2 μg) and can be modeled as a linear arrangement of FDH molecules trapped between the CNTs (Figure 2c). At higher contents of FDH, the current values decreased, probably because the overloaded enzymes failed to interface effectively with the CNTs. To investigate enzyme activity within the e^2CNTF films, the apparent Michaelis−Menten constant ($K_{m,app}$) was estimated from the currents at various fructose concentrations using the Lineweaver−Burke equation[24,25] (Figure 5). The derived $K_{m,app}$ was around 10 mM, which is in agreement with the K_m value for the reaction in the bulk solution,[26] indicating that the nanospace formed by CNTF shrinkage could maintain the nature of the FDH enzyme.

Construction of Biofuel Cells. To construct biofuel cells using a FDH-based anode, we prepared a LAC-entrapped CNTF

dx.doi.org/10.1021/ja111517e |J. Am. Chem. Soc. 2011, 133, 5129–5134

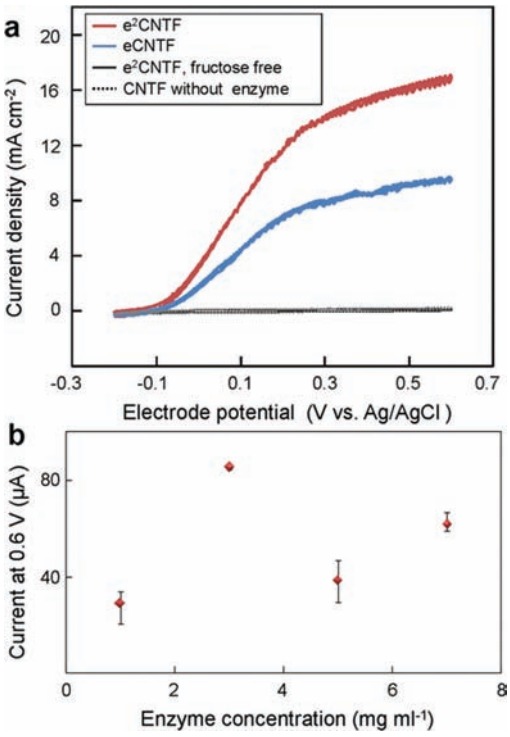

Figure 4. (a) Cyclic voltammograms at 10 mV s^{-1} in the stirred buffer containing 200 mM fructose for the enzyme-adsorbed as-grown CNTF (eCNTF) and the enzyme-entrapped CNTF (e^2CNTF); both were prepared using 12 μm thick CNTF films and 3 mg mL^{-1} FDH solution. The control experiments (enzyme-free or fructose-free) are also shown. The area of one side of the film (1 mm^2 for eCNTF and 0.5 mm^2 for e^2CNTF) was used to the calculation of current density, as validated in the Experimental Section (Electrochemical Measurements) by using Supporting Information, Figure S2. (b) Currents at 0.6 V vs Ag/AgCl of the e^2CNTF films prepared from FDH solutions of different concentrations. The experiments were carried out three times for each condition.

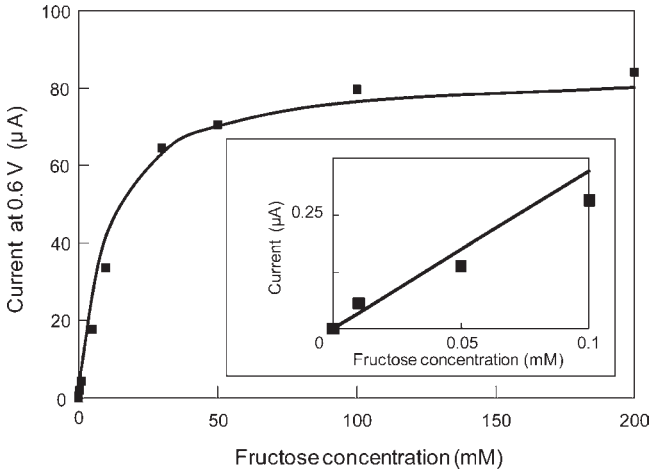

Figure 5. The oxidation currents as a function of the fructose concentration, measured at 0.6 V vs Ag/AgCl in stirred McIlvaine buffer (pH 5.0) for the e^2CNTF electrode prepared using a 12 μm thick CNTF and 3 mg mL^{-1} FDH solution.

cathode for O_2 reduction. The optimized LAC solution (0.25 mg mL^{-1}) was perfused into a 20 μm thick CNTF film, followed by shrinkage to one-third of the original area (~0.3 mm^2). Cyclic voltammograms of the e^2CNTF showed O_2 reduction at a potential more negative than 0.67 V with a maximum current density of ca. 2 mA cm^{-2} in stirred condition (Figure 6a). From the separate 7 experiments using different LAC-e^2CNTF electrodes, the average of current density was found to be 2.1 ± 0.3 mA cm^{-2}. A further increase in current density to ca. 4 mA cm^{-2} was achieved by overlapping two pieces of e^2CNTF by taking advantage of their free-standing character. By connecting this cathode with the FDH-based anode (Figure 6b), the fuel cell performance was evaluated in an O_2-saturated McIlvaine buffer containing 200 mM fructose. Figure 6c shows the typical power−voltage and current−voltage curves plotted on the basis of the cell voltage upon changing the external resistance (1 kΩ ~ 2 MΩ). The open-circuit voltage of the cell was 0.77 V in agreement with the difference between the potentials at which fructose oxidation and oxygen reduction start to occur on cyclic voltammetries (−0.1 V in Figure 4a and 0.67 V in Figure 6a, respectively). The maximum current density of the cell was ca. 4.8 mA cm^{-2} by reflecting the performance of the present LAC-based cathode. The power density reached 1.8 mW cm^{-2} (at 0.45 V) in stirred condition, 84% of which could be maintained after continuous operation for 24 h, as shown in Figure 6d.

Application of Enzyme−CNTF Ensemble Films To Power a LED Device. The "free-standing and flexible" character of the present enzyme electrode is its most attractive advantage from a practical viewpoint. The application of such e^2CNTF electrodes for flexible and miniature biodevices is demonstrated in Figure 7. Pieces of e^2CNTF films were patched on an O_2 plasma-treated gold pattern on a polyethylene terephthalate (PET) substrate. After being air dried, the e^2CNTF films remained attached while being bent and immersed in a solution. Similarly, the e^2CNTF films can be wound on the electric leads of a light-emitting diode (LED) device, whose blinking interval is inversely proportional to the power of the biofuel cell. The leads of the LED device were immersed in O_2-saturated stirred McIlvaine buffer (pH 5.0) containing 200 mM fructose. The blinking interval of the LED driven by the e^2CNTF-wound anode and cathode (0.24 s) was similar to that when the e^2CNTF film were merely clamped on the leads without winding (0.20 s), which indicates that the e^2CNTF electrodes maintained their performance in the stressed wound conditions. This unique e^2CNTF-wound needle-type bioelectrode will also be applicable to advanced biosensors and medical devices.[27,28]

CONCLUSION

The results presented here show the controlled entrapment of enzymes inside CNTF films through liquid-induced shrinkage. This provides a first example of an enzyme electrode that automatically regulates its intrananospace in response to enzymes to be immobilized. The proposed "in-situ regulation" is a straightforward approach to avoid the longstanding difficulty in the postmodification of enzymes into conventional nanostructured electrodes. In addition, the prepared e^2CNTF film is the first free-standing, flexible enzyme electrode. We demonstrate its use in miniature biofuel cells in patch and wound forms. This free-standing character should also be a significant advantage for other miniature biodevices, such as biosensors. The e^2CNTF film electrodes exhibited reproducible activity in the mA cm^{-2} range. The biofuel cells with e^2CNTF films retained ~80% output at

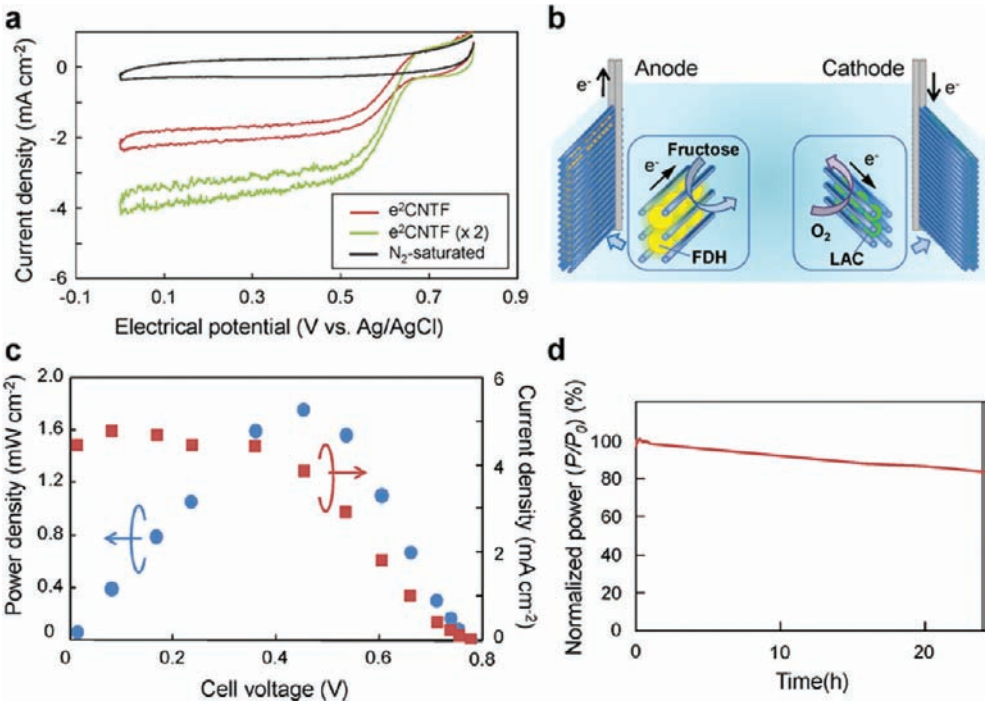

Figure 6. (a) Typical cyclic voltammograms of LAC-entrapped e^2CNTF films (single piece and overlapped double pieces) at 10 mVs^{-1} in O_2-saturated stirred McIlvaine buffer (pH 5.0). The electrode films were prepared using 20 μm thick CNTF film and 0.25 mg mL^{-1} LAC solution. The area of one side of the e^2CNTF film (0.3 mm^2 for both single and overlapped double films) was used for the calculation of current density, as validated in the Experimental Section (Electrochemical Measurements) by using Supporting Information, Figure S2. (b) Schematic of e^2CNTF-based biofuel cell structure. (c) Performance of a biofuel cell composed of a FDH−e^2CNTF anode and the LAC−e^2CNTF cathode in O_2-saturated stirred McIlvaine buffer (pH 5.0) containing 200 mM fructose. The area of one side of the cathode film (0.3 mm^2) was used for the calculation of current and power densities. (d) Dependence of relative stability of power (%) on time with external load of 35.3 kΩ, which is the condition for the maximum power in (c).

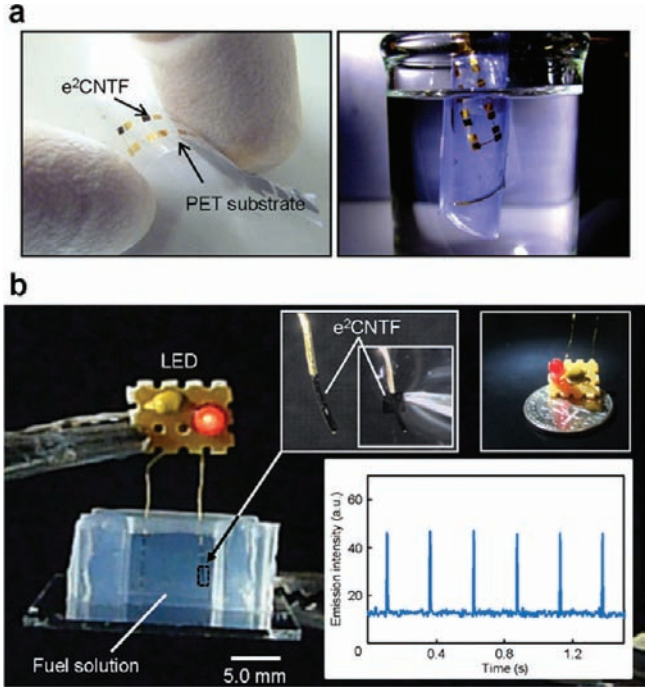

Figure 7. (a) Photographs of e^2CNTF films patched to a flexible PET substrate. The films remained attached while being rolled and immersed in water. (b) Photographs of e^2CNTF films wound on the electric leads of the LED device. The inset shows the time course of the emission intensity of an LED driven by the e^2CNTF-wound anode and cathode.

the mW cm^{-2} level for more than 1 day. To further enhance the cell performance, we intend to create end and sidewall openings in the CNTs by preheating to 600 °C,[17] allowing more efficient flow through the CNTF. The present in situ regulation approach is also applicable for co-entrapment of multiple kinds of enzymes for multifuel or multistep oxidation systems.[29,30]

■ ASSOCIATED CONTENT

Ⓢ Supporting Information. Details of the synthesized CNTF (PDF), a movie of LED emission (MPG), and data of electrochemical measurement (PDF). This material is available free of charge via the Internet at http://pubs.acs.org.

■ AUTHOR INFORMATION

Corresponding Author
nishizawa@biomems.mech.tohoku.ac.jp

■ ACKNOWLEDGMENT

This work was supported by a Core Research for Evolutional Science and Technology grant from the Japan Science and Technology Agency and by a Grant-in-Aid for Creative Scientific Research (Creation of Nano Energetic Systems) from the Ministry of Education, Science and Culture, Japan.

REFERENCES

(1) Mano, N.; Mao, F.; Heller, A. *J. Am. Chem. Soc.* **2003**, *125*, 6588–6594.
(2) Bullen, R. A.; Arnot, T. C.; Lakeman, J. B.; Walsh, F. C. *Biosens. Bioelectr.* **2006**, *21*, 2015–2045.
(3) Kim, J.; Jia, H.; Wang, P. *Biotechnol. Adv.* **2006**, *24*, 296–308.
(4) Wang, J.; Lin, Y. *TrAC, Trends Anal. Chem.* **2008**, *27*, 619–626.
(5) Willner, I.; Yan, Y. M.; Willner, B.; Tel-Vered, R. *Fuel Cells* **2009**, *1*, 7–24.
(6) Gellett, W.; Kesmez, M; Schumacher, J.; Akers, N.; Minteer, S. D. *Electroanalysis* **2010**, *22*, 727–731.
(7) Togo, M.; Takamura, A.; Asai, T.; Kaji, H.; Nishizawa, M. J. *Power Sources* **2008**, *178*, 53–58.
(8) Miyake, T.; Oike, M.; Yoshino, S.; Yatagawa, Y.; Haneda, K.; Nishizawa, M. *Lab Chip* **2010**, *10*, 2574–2578.
(9) Moehlenbrock, M. J.; Minteer, S. D. *Chem. Soc. Rev.* **2008**, *37*, 1188–1196.
(10) Katz, E.; Willner, I. *Chem. Phys. Chem.* **2004**, *5*, 1084–1104.
(11) Gao, F.; Viry, L.; Maugey, M.; Poulin, P.; Mano, N. *Nat. Commun.* **2010**, *1*, 2.
(12) Kamitaka, Y.; Tsujimura, S.; Setoyama, N.; Kajino, T.; Kano, K. *Phys. Chem. Chem. Phys.* **2007**, *9*, 1793–1801.
(13) Sakai, H.; Nakagawa, T.; Tokita, Y.; Hatazawa, T.; Ikeda, T.; Tsujimura, S.; Kano, K. *Energy Environ. Sci.* **2009**, *2*, 133–138.
(14) Tsujimura, S.; Nishina, A.; Hamano, Y.; Kano, K.; Shiraishi, S. *Electrochem. Commun.* **2010**, *12*, 446–449.
(15) Hata, K.; Futaba, D. N.; Mizuno, K.; Namai, T.; Yumura, M.; Iijima, S. *Science* **2004**, *306*, 1362–1364.
(16) Futaba, D. N.; Hata, K.; Yamada, T.; Hiraoka, T.; Hayamizu, Y.; Kakudate, Y.; Tanaike, O.; Hatori, H.; Yumura, M.; Iijima, S. *Nat. Mater.* **2006**, *5*, 987–994.
(17) Hiraoka, T.; Izadi-Najafabadi, A.; Yamada, T.; Futaba, D. N.; Yasuda, S.; Tanaike, O.; Hatori, H.; Yumura, M.; Iijima, S.; Hata, K. *Adv. Funct. Mater.* **2010**, *20*, 422–428.
(18) Fournier, J.; Miousse, D.; Brossard, L.; Menard, H. *Mater. Chem. Phys.* **1995**, *42*, 181–187.
(19) Losic, D.; Shapter, J. G.; Gooding, J. J. *Langmuir* **2002**, *18*, 5422–5428.
(20) Tominaga, M.; Shirakihara, C.; Taniguchi, I. *J. Electroanal. Chem.* **2007**, *610*, 1–8.
(21) Piontek, K.; Antorini, M.; Choinowski, T. *J. Biol. Chem.* **2002**, *277*, 37663–37669.
(22) Wu, X.; Zhao, F.; Varcoe, J. R.; Thumser, A. E.; Avignone-Rossa, C.; Slade, R. C. T. *Biosens. Bioelectr.* **2009**, *25*, 326–331.
(23) Zhao, X.; Jia, H.; Kim, J.; Wang, P. *Biotechnol. Bioeng.* **2009**, *104*, 1068–1074.
(24) Kamin, R. A.; Wilson, G. S. *Anal. Chem.* **1980**, *52*, 1198–1205.
(25) Tominaga, M.; Nomura, S.; Taniguchi, I. *Biosens. Bioelectr.* **2009**, *24*, 1184–1188.
(26) Ameyama, M.; Shinagawa, E.; Matsushita, K.; Adachi, O. *J. Bacteriol.* **1981**, *145*, 814–823.
(27) Heller, A.; Feldman, B. *Chem. Rev.* **2008**, *108*, 2482–2505.
(28) Wei, X.; Liu, J. *Front Energy Power Eng. China* **2008**, *2*, 1–13.
(29) Palmore, G. T. R.; Bertschy, H.; Bergens, S. H.; Whitesides, G. M. *J. Electroanal. Chem.* **1998**, *443*, 155–161.
(30) Arechederra, R. L.; Minteer, S. D. *Fuel Cells* **2009**, *1*, 63–69.